

# Performance of Critical Flow Venturis under Transient Conditions

John D. Wright  
NIST Fluid Metrology Group  
100 Bureau Drive, Mail Stop 8361  
(301) 975-5937 voice, (301) 258-9201 fax, [john.wright@nist.gov](mailto:john.wright@nist.gov)

**Abstract:** Critical flow venturis (CFVs) can be used to measure flow under transient pressure and flow conditions with uncertainties of 0.13 % or less (95 % confidence level). Blow-down tests transferred 630 g of nitrogen during a 100 s interval from an unregulated cylinder (initially at 10 MPa) through a heat exchanger and a CFV into a known collection volume. Fast pressure and temperature sensors were used to calculate the CFV flow. The integrated CFV mass flows,  $\int \dot{m} dt$ , averaged 0.04 % smaller than the mass  $\Delta\rho V$  of the collected gas. The heat exchanger was essential to the excellent agreement; without it, the percentage difference between  $\int \dot{m} dt$  and  $\Delta\rho V$  was 0.38 %. We conclude that even under transient conditions, a properly instrumented CFV can be used as a reference flowmeter to evaluate other flowmeter types or to test gaseous fuel dispensers in the field.

## 1. INTRODUCTION

Flowmeter calibrations are normally conducted under steady-state pressure, temperature, and flow conditions, but in many applications, the meters are used under unsteady conditions. Unfortunately, transients may introduce large flow errors and the effects of transients on various meter types are not well known. An important unsteady application of current interest is the refueling of vehicles with natural gas or hydrogen.

Figure 1 shows a typical arrangement for a hydrogen gas dispenser. A compressor uses gas from a low pressure source to fill a set of pressure vessels (a cascade tube bank). Valves are sequentially opened to allow gas to flow from each cascade tube to the vehicle tank. As each tube is opened, surges of flow and pressure occur at the flowmeter in the dispenser (e.g. a coriolis flowmeter). Wide temperature changes also occur at the flowmeter. Consumers and inspectors expect < 2 % accuracy from gaseous fuel dispensers, but errors > 10 % have been reported. At natural gas refueling stations, turbine meters subjected to pulsatile flow over-reported totalized flow by as much as 15% [1].

NIST is constructing a calibration facility to generate accurately measured transient flows so that flowmeter performance under unsteady conditions can be evaluated and improved. The transient flows will be generated by sequentially opening valves on high pressure cylinders. In the absence of a regulator and heat exchanger, the meter under test will be exposed to rapid changes

in pressure, temperature, and flow, mimicking the conditions found in gaseous fuel dispenser applications. The reference flowmeters in the NIST facility will be critical flow venturis (CFVs) [2], previously calibrated by our existing steady-flow PVTt standards [3].

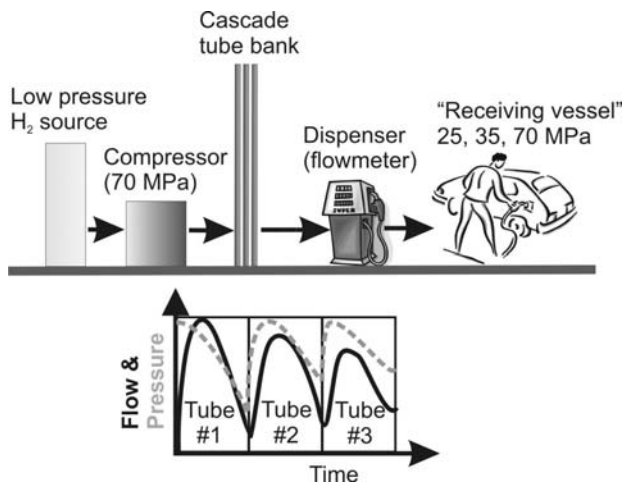


**Fig. 1** Schematic of a gaseous fuel dispenser using a cascade tube bank. Flow, pressure, and temperature are all transient at the flowmeter in the dispenser, leading to significant billing errors.

Critical flow venturis can act as accurate flow standards in transient applications. To first order, the response time of a CFV equals a characteristic length (e.g. throat diameter) divided by the speed of sound; this time is approximately 1  $\mu$ s for the 1 mm

CFV we are using.\* In practice, the response time of a CFV is limited by the time constants of the pressure and temperature sensors associated with the CFV. Pressure and temperature sensors with time constants < 100 ms are available. The purpose of this work is to demonstrate the ability of properly instrumented CFVs to accurately measure flow under transient conditions.

Once the accuracy of CFVs under transient conditions is demonstrated, they will be valuable tools for laboratory evaluations of other flowmeter types considered for transient applications. Also, CFVs can be used by weights and measures inspectors as “master meters”, field standards used to test compliance of gaseous fuel dispensers with accuracy regulations.

## 2. GENERAL DESCRIPTION OF THE EXPERIMENT

To demonstrate the ability of CFVs to accurately measure transient flows, we 1) calibrated a 1 mm diameter CFV under steady temperature, pressure, and flow conditions at pressures up to 13 MPa, 2) instrumented the CFV with fast pressure and temperature sensors and a fast data acquisition system, and 3) conducted blow-down tests to check that the integrated CFV flow agrees with the mass of gas collected in a collection volume (see Figure 2).

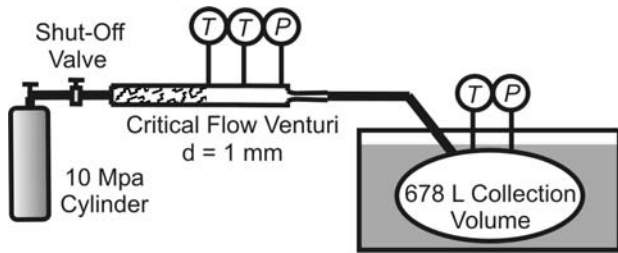


**Fig. 2** A schematic of a blow-down test arrangement to study CFV transient performance.

\* There are second order effects on CFV flows that are much slower. For example, after a flow change, a long time interval is required to attain a steady temperature distribution in the CFV body. During this interval, the changing thermal boundary layer in the CFV generates a small, time-dependence of the discharge coefficient.



**Fig. 3** The temperature controlled 678 L collection volume.

For the blow-down tests, an 8 L cylinder was pressurized with nitrogen to 10 MPa. The pressurized cylinder was the source of gas for the 1 mm CFV. The discharge from the CFV was collected in a 678 L volume, part of a NIST *PVTt* flow standard (see Figure 3). The collection volume and the piping downstream from the shut-off valve were evacuated to < 20 Pa and initial pressure and temperature values were recorded ( $P_i$  and  $T_i$ ). The fast data acquisition system was activated to record the pressure and the temperature at the inlet of the CFV every 50 ms. The shut-off valve was opened for approximately 100 s allowing gas to flow from the pressure vessel into the collection volume. After the pressure in the cylinder fell to approximately 900 kPa, the shut-off valve was closed. After the pressure and temperature in the collection volume and piping reached equilibrium, we recorded the final values  $P_f$  and  $T_f$ . The mass of gas collected in the tank was calculated via the equation:

$$m_T = V(\rho_f - \rho_i) \quad (1)$$

where  $V$  is the volume of the tank and piping downstream from the CFV (678.726 L),  $\rho_i$  is the initial gas density, and  $\rho_f$  is the final gas density. The gas density was calculated via a real gas

equation of state [4]. The final pressure in the collection volume was approximately 80 kPa, and the mass of nitrogen collected was 630 g. The collection volume was in a temperature controlled water bath, so that the measurement of the temperature of the collected gas had uncertainty of 12 mK ( $k = 2$ ) \* [3].

The mass of gas that flowed through the CFV into the collection volume was calculated by numerically integrating the CFV flow during the time interval when the shut-off valve was open:

$$m_{\text{CFV}} = \int_{t_i}^{t_f} \dot{m}_{\text{CFV}} dt \cong \sum_{k=1}^{n-1} \frac{\dot{m}_k + \dot{m}_{k+1}}{2} (t_{k+1} - t_k) \quad (2)$$

where  $t_i$  and  $t_f$  are initial and final times that span the interval that the shut-off valve was open,  $t_k$  are the times at which  $n$  discrete CFV flow measurements covering the open valve period were made, and the CFV mass flow is given by:

$$\dot{m}_{\text{CFV}} = \frac{C_d P_0 A C^* \sqrt{\mathcal{M}}}{\sqrt{RT_0}} \quad (3)$$

where  $C_d$  is the CFV discharge coefficient,  $P_0$  and  $T_0$  are the stagnation pressure and temperature,  $A$  is the throat area,  $C^*$  is the real gas critical flow function [4],  $\mathcal{M}$  is the molecular mass, and  $R$  is the universal gas constant. If the CFV accurately measures flow through transient conditions, then the mass accumulated in the collection volume will equal the integrated CFV flow, i.e.  $\Delta\rho V = \int \dot{m} dt$ .

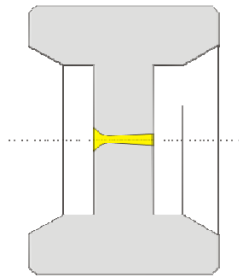


**Fig. 4** CFV machined into a high pressure taper seal fitting.

### 3. EXPERIMENTAL DETAILS

\*  $k = 2$ , i.e. approximately 95 % confidence level value.

The 1 mm CFV was machined into a 60 ° taper seal high pressure fitting for 25 mm tubing (see Figure 4). The approach tube for the CFV was 70 cm long with inside diameter of 14 mm and the tube exterior was insulated (see Figure 5). The first half of the approach tube was filled with brass wool to promote temperature uniformity across the pipe cross section and to break up the jet resulting from the expansion from 5 mm to 14 mm inside diameters at the approach tube inlet (see Figure 2).

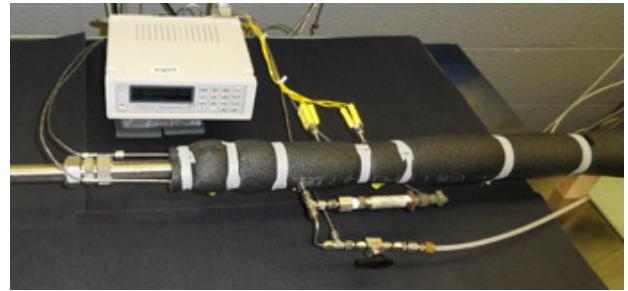


**Fig. 5** A photograph of the CFV test section for the blow-down tests.

The approach tube had three ports, one for a pressure tap and two for temperature sensors, 23 cm and 16 cm upstream from the CFV inlet. The temperature sensors were exposed Type K thermocouples with wire diameter of 0.05 mm welded onto 0.25 mm supports within a 3 mm insertion tube. Two thermocouple junctions were installed within each 3 mm insertion tube (see Figure 6). The time constant of the thermocouples ranges from 20 ms to 100 ms depending on the flow of gas [5].



**Fig. 6** 0.05 mm thermocouple pair.

Even with insulation on the flow tube, heat transfer from the room causes the gas temperature to

change as it approaches the CFV. Obtaining accurate CFV gas temperature measurements is a major source of uncertainty in some applications (see Section 8). In these experiments, the two temperature measurements from the streamwise displaced sensors were extrapolated to obtain the temperature at the plane of the CFV inlet and this temperature was used for all CFV calibrations and flow calculations, *i.e.*,

$$T_1 = tc_2 + \frac{16}{7}(tc_2 - tc_1) \quad (4)$$

where  $T_1$  is the CFV static temperature,  $tc_1$  and  $tc_2$  are the temperatures measured by thermocouples 1 and 2, and the distances between thermocouples 1 and 2 is 7 cm and the thermocouple 3 is 16 cm from the CFV entrance.  $T_1$  was used to calculate the stagnation temperature  $T_0$  using the corrections found in reference [2]. The difference between  $T_1$  and  $T_0$  was less than 1 part in  $10^6$  for all the tests shown herein.

The manufacturer's specification for the pressure sensor time constant is 3 ms. However, the flow impedance imposed by the pressure tap and tubing between the approach tube and the transducer can slow the time response. Experiments and analytical estimates give a time constant of < 10 ms. During transient tests, data were acquired in 20 s bursts with 50 ms resolution.

Slow pressure sensors were installed in parallel with the fast sensors and they were used under steady-state conditions to re-zero the fast sensors before each test. Slow temperature sensors (3 mm sheathed thermistors) were used to measure the temperature at the external surface of the CFV body.

#### 4. STEADY-STATE CFV CALIBRATIONS

The CFV was calibrated with > 99.995% purity nitrogen using the NIST 34 L and 678 L *PVTt* flow standards to obtain  $C_d$  values at Reynolds numbers between  $25 \times 10^3$  and  $1.4 \times 10^6$ , covering the range that would occur during the blow-down tests when the pressure dropped from 10 MPa to 200 kPa. The calibrations were performed under approximately steady-state conditions using the test arrangement shown in Figure 7. The source of nitrogen was a manifold of 8 cylinders filled to 41 MPa. The regulator was used to maintain pressure at the

desired set point. A stirred water bath controlled to match room temperature and 5 m of coiled stainless steel 6.4 mm tubing immersed in the water served as a heat exchanger to return the cold gas exiting the regulator to room temperature. The output from the CFV was connected to the NIST *PVTt* standards which measured mass flow with 0.025 % ( $k = 2$ ) uncertainty [6].

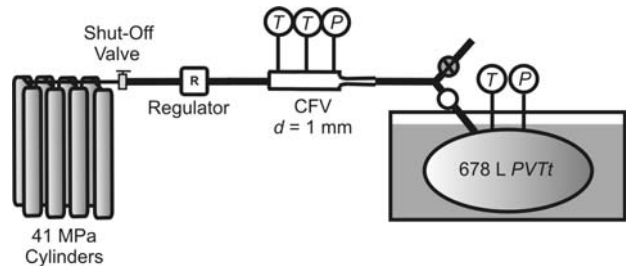


**Fig. 7** Schematic of equipment used for calibration of the CFV under steady-state conditions.

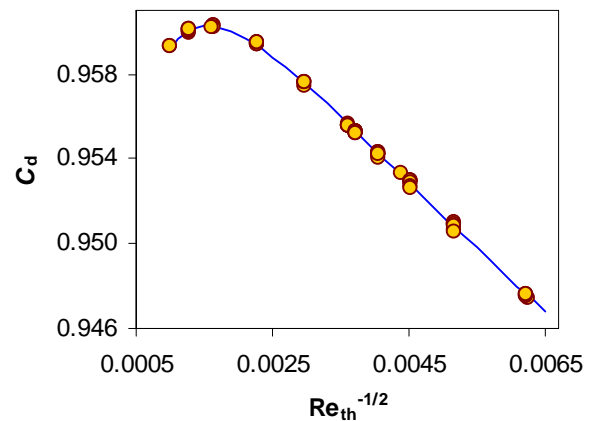


**Fig. 8** Discharge coefficient versus the inverse square root of Reynolds number. Laminar to turbulent transition occurs at the lower  $Re_{th}^{-1/2}$  values. A constant throat diameter of 1 mm was assumed for these calculations.

A plot of  $C_d$  versus the inverse square root of the theoretical Reynolds number for the 1 mm CFV is shown in Figure 8 along with a best fit curve used to calculate  $C_d$  for the CFV flow measurements. The theoretical Reynolds number is calculated using the theoretical mass flow, *i.e.* using  $C_d = 1$  in Equation 3. At  $Re_{th}$  of approximately  $4 \times 10^5$  ( $Re_{th}^{-1/2} = 0.0016$ ), the  $C_d$  curve departs from linearity due to the laminar to turbulent transition of the boundary layer [7]. A rational function (a quotient of 2 second

order polynomials) was used to predict  $C_d$  for a given  $Re_{th}$  during the blow-down tests.

## 5. COMPARISONS OF INTEGRATED CFV MASS $\int \dot{m} dt$ AND COLLECTED MASS $\Delta\rho V$

### 5.1 Steady-State Temperature and Pressure

The data reduction software that compares  $\int \dot{m} dt$  and  $\Delta\rho V$  was tested under steady-state temperature, pressure, and flow conditions before using it to analyze transient flows. A pressure regulator and heat exchanger were placed between the gas source and the CFV as shown in Figure 9.

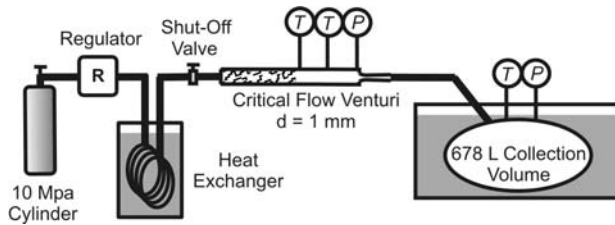


**Fig. 9** Test arrangement for steady-state flow tests.

In this test, the integrated mass flow from the CFV agreed with the mass collected in the  $PVTt$  tank within 0.01 %. This is expected because the same collection volume was used to measure the steady-state  $C_d$  values and to measure  $\Delta\rho V$ ; however, this test is essential to validate the algorithms used for CFV flow calculations and their integration.

### 5.2 Steady-State Temperature, Transient Pressure

In the next set of experiments,  $\int \dot{m} dt$  and  $\Delta\rho V$  were compared using the equipment shown in Figure 10, *i.e.* with a heat exchanger between the blow-down tank and the CFV approach tube.

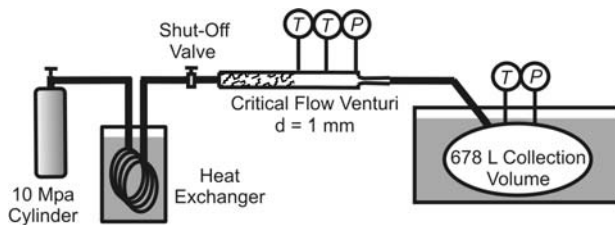


**Fig. 10** Test arrangement for steady-state temperature, transient pressure tests.

Except for 2 s long spikes caused by opening and closing the shut-off valve, the heat exchanger maintained the CFV gas temperature at  $294.5 \text{ K} \pm 1 \text{ K}$  during the filling process. Four steady-state-temperature / transient-pressure tests were performed. The differences between  $\int \dot{m} dt$  and  $\Delta\rho V$  for the four tests averaged +0.04 % with standard deviation of 0.04 %.

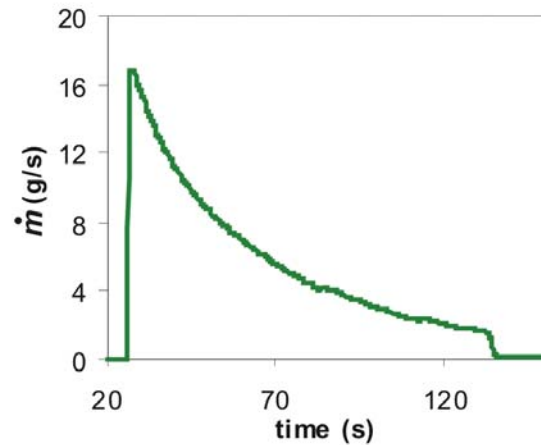


**Fig. 11** Mass flow calculated from the CFV during a transient  $T$  and  $P$  blow-down test.

### 5.3 Transient Temperature and Pressure

In the next set of transient experiments, both the heat exchanger and the regulator were removed as depicted in Figure 2. Hence, both temperature and pressure dropped dramatically as the blow-down tank emptied. Figure 11 shows the mass flow measured by the CFV for one of these tests in which the difference between  $\int \dot{m} dt$  and  $\Delta\rho V$  was  $-0.39 \%$ .

The pressures and temperatures measured with the fast sensors are plotted in Figures 12 and 13. Opening the shut-off valve causes a rapid increase in pressure and an upward temperature spike due to heat of compression. A similar downward temperature spike occurs when the shut-off valve is closed. The thermocouple measurements used to calculate  $T_0$  are also plotted in Figures 12 and 13.

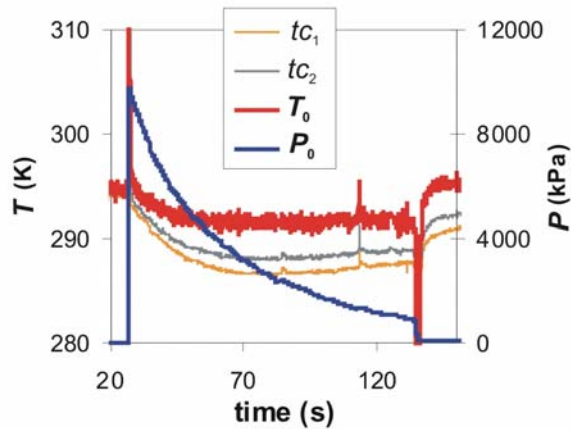


**Fig. 12** CFV pressure and temperature during a transient  $T$  and  $P$  blow-down test.  $T_0$  is the stagnation temperature at the CFV inlet (calculated from  $T_1$ ).

Our results are remarkably sensitive to the measurement of the temperature  $T_1$  of the gas at the CFV's inlet. For example, if one assumed  $T_1 = tc_1$  instead of using Equation 4, the difference between  $\int \dot{m} dt$  and  $\Delta\rho V$  would be +0.31 % instead of -0.39 %.

The transient temperature and pressure test was repeated four times and the average difference between  $\int \dot{m} dt$  and  $\Delta\rho V$  was -0.38 % with a standard deviation of 0.01 %.

## 6. UNCERTAINTY OF THE DIFFERENCE $\int \dot{m} dt - \Delta\rho V$

Table 1 lists four major categories of the uncertainty sources for the difference between  $\int \dot{m} dt$  and  $\Delta\rho V$  for the transient experiments. We will discuss the uncertainty components here and in following sections consider why the results of the transient temperature tests are worse than expected.

A) PVTt calibration includes the uncertainty of the flow standard used to calibrate the CFV as well as uncertainties in the pressure and temperature instrumentation used during the calibration.

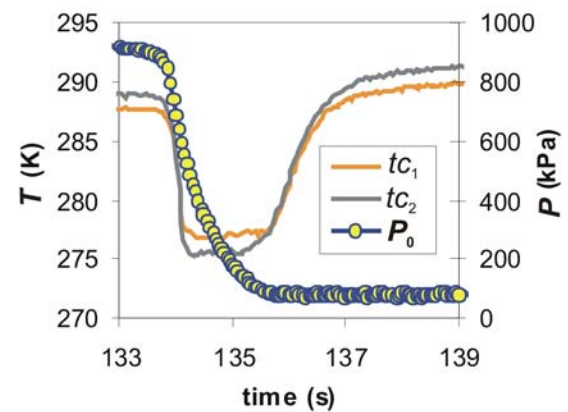
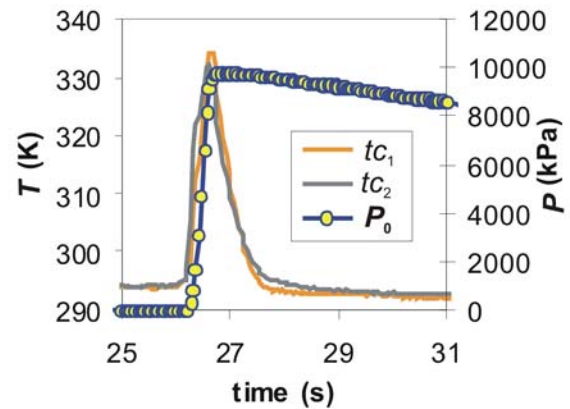


**Fig. 13** Zoomed views of the test start and stop intervals showing pressure and thermocouple temperature measurements used to calculate  $T_0$ .

B) CFV mass flow comprises uncertainties of the CFV when used to measure flow during the transient tests. The  $C_d A$  stability component accounts for offsets in  $C_d A$  observed between periodic calibrations. We suspect that the changes resulted from opening and closing the high pressure taper seal fitting. Different torques applied in closing the fitting lead to different stress on the CFV body that change the CFV throat diameter.

Different pressure and temperature sensors were used during CFV calibration and usage, hence instrumentation uncertainties appear again in this category along with response time uncertainties. Because the total integration time is  $> 100$  s and the  $P$  and  $T$  sensor time constants are  $< 100$  ms, the response time is not a significant uncertainty component for this experiment. Uncertainties in  $C^*$  are negligible because they are correlated between CFV calibration and usage. Care was taken to maintain the nitrogen purity, so molecular mass uncertainty is not significant.

C) **Integration:** Time labels in data files were based on a computer clock. The clock was checked against the NIST time reference and found correct to 7 parts in  $10^6$ . Numerical errors caused by using the trapezoidal rule were estimated. Also, there are intervals at the start and stop of up to 300 ms during which the pressure is less than 150 kPa and the CFV is not under critical flow conditions. These intervals were not included in the numerical integration; however during these intervals, gas moved through the CFV into the collection volume. Equation 3 will over-report the mass flow during these non-critical conditions. By including the non-critical intervals in the numerical integration, we obtained an estimate of the uncertainty from the “non-critical tails”.

Table 1. Uncertainty for the difference  $\int \dot{m} dt - \Delta\rho V$  for the transient temperature and pressure test.

Uncertainty Component	Normalized Sensitivity (-)	Uncertainty ( $k = 1$ , %)
<b>A) PVTt calibration</b>		
1. PVTt standard	1	0.013
2. $P$	1	0.020
3. $T$	0.5	0.010
<b>B) CFV mass flow</b>		
4. $C_d A$ stability	1	0.025
5. $P$	1	0.050
6. $T$	0.5	0.010
7. $P$ and $T$ response time	1	0.010
8. $C^*$	1	< 0.001
9. $R, \mathcal{M}$	0.5	< 0.001
<b>C) Integration</b>		
10. Time	1	< 0.001
11. Numerical errors	1	0.005
12. Non-critical tails	1	0.005
<b>D) <math>\Delta\rho V</math></b>		
13. $\Delta\rho$	1	0.007
14. $V$	1	0.010
<b>Combined Unc. (<math>k = 1</math>)</b>		<b>0.06</b>
<b>Expanded Unc. (<math>k = 2</math>)</b>		<b>0.13</b>

Normalized sensitivity coefficients are unity for most components but are  $\frac{1}{2}$  for the quantities under the square root in the CFV mass flow equation. Based on this analysis, we expect agreement between  $\int \dot{m} dt$  and  $\Delta\rho V$  to be within 0.13 % ( $k = 2$ ). Hence, the differences measured during the steady-state temperature, transient pressure tests (0.04 %) are within uncertainty expectations, but the transient

temperature and pressure results (-0.038 %) exceed the expected uncertainty

This raises the question, which uncertainty components are missing or underestimated in the analysis? The relatively long 100 s time scale of the tests leads to the conclusion that the differences are not due to the pressure and temperature sensor time constants. Because the differences are much larger than the differences for the steady-state-temperature / transient-pressure tests, temperature measurement problems are probably the source of the error. We explore the two most likely sources in the following sections.

## 7. THERMAL EFFECTS ON $C_d A$

Prior researchers have observed changes in the flow discharged from a CFV as a function of time after start-up, presumably due to the CFV gradually reaching thermal equilibrium with the gas [8]. There are two thermal effects: 1) thermal expansion of the CFV material changes its throat area  $A$ , and 2) the CFV wall temperature affects the mass flux of gas in the thermal boundary layer [9, 10].

During long, steady-state calibrations, the body temperature for the 1 mm CFV decreased to 273 K (see Figure 15). For this temperature change, thermal expansion effects on the throat area are -0.07 %, less than a quarter of the observed differences between  $\int \dot{m} dt$  and  $\Delta\rho V$ . The transient tests lasted only 100 s, not long enough for the CFV temperature to fall as low as 273 K, so thermal expansion effects will be even smaller than -0.07 % and cannot explain the -0.38 % differences observed in the transient temperature tests.

According to reference [9], for the Reynolds numbers in the blow-down tests herein, thermal boundary layer effects are < 0.05 %. They are too small, of opposite polarity, and cannot explain the observed differences between  $\int \dot{m} dt$  and  $\Delta\rho V$  either.

## 8. CFV TEMPERATURE MEASUREMENT ERRORS

Perhaps the most surprising outcome of the present research is the degree that widely used temperature measurement methods can contribute to the uncertainty of CFV flow measurements.

$$* \Delta A/A = 2\alpha(\Delta T) = (34 \times 10^{-6} / ^\circ\text{C})(-20 ^\circ\text{C}) = -0.07 \%$$

Large temperature gradients often occur in the piping and gas near a CFV and this leads to sampling uncertainties and significant errors in the stagnation temperature,  $T_0$ .

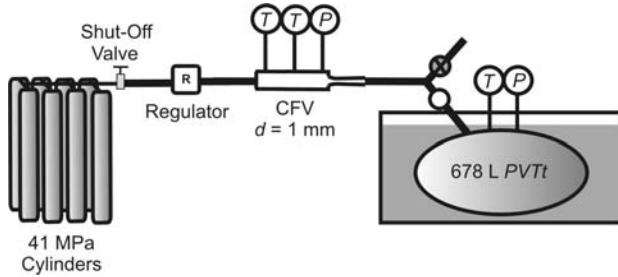


**Fig. 14** Test set up used to investigate temperature measurement uncertainties in CFVs.

The arrangement shown in Figure 14 was used to demonstrate the problem. The 678 L PVTt standard was used to measure  $C_d A$  values for the 1 mm CFV. A 3 mm sheathed thermistor was installed at the upstream temperature tap and a pair of fast thermocouples as described in Section 3 were installed at the downstream tap. Also, a thermistor was placed in contact with the CFV body, under a layer of insulation (as in Figure 5).

Temperature traces and  $C_d A$  values are shown in Figure 15. Flow was continuous but  $C_d A$  values are separated by 50 min mostly due to the time required to evacuate and stabilize conditions in the PVTt collection tank: the fill times are only 133 s. In this test, the CFV pressure was regulated to be  $3.2 \text{ MPa} \pm 0.1 \text{ MPa}$ . Initially, cold gas due its expansion from 41 MPa to 3.2 MPa at the regulator leads to a rapid drop in all temperatures. As the gas pressure in the source cylinders drops, the cooling capacity of the gas exiting the regulator decreases. Hence, after about 50 min, all temperatures increase.

A second gas expansion occurs through the CFV, cooling the CFV body. The cold CFV body cools the upstream piping by conduction which, in turn, cools the gas at the temperature sensors. The thermistor and thermocouple are both mounted on the approach tube centerline, separated by 7 cm, but they differ by as much as 7 K, due to differences in their time constants and stem conduction errors in the thermistor. In summary, there are large, time-dependent, axial and radial temperature gradients in the approach tube.

To illustrate the errors this introduces, the  $C_d A$  values resulting from using the thermistor and

thermocouple readings are plotted in Figure 15 and they differ by as much as 0.6 %. This example demonstrates that it can be challenging to obtain an accurate measurement of the temperature of the gas immediately upstream from the CFV. In this work, we extrapolated the readings of two thermocouples displaced in the streamwise direction, but more sophisticated approaches are needed because temperature measurement errors are a major uncertainty contributor to CFV flow measurements.

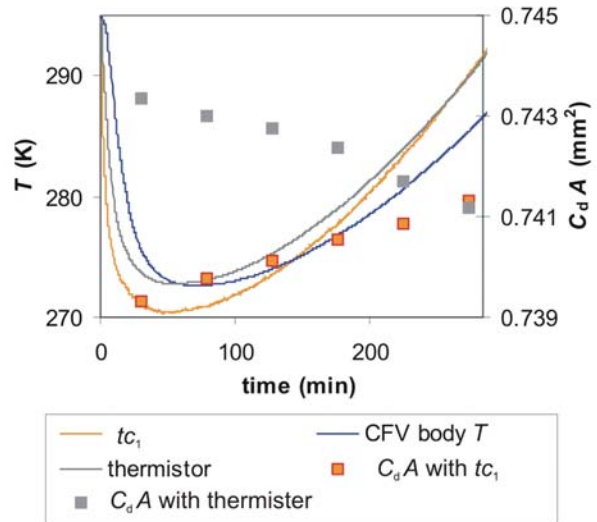


**Fig. 15** Temperature traces and  $C_d A$  values for a PVTt CFV calibration without a heat exchanger, illustrating  $C_d A$  differences due to different temperature measurement methods.

## 9. CONCLUSIONS

Blow-down tests confirm that critical flow venturis accurately measure flow under transient conditions. Under transient pressure and temperature conditions, we obtained agreement of -0.38 % between numerically integrated CFV flows and the mass accumulated in a collection volume. Under transient-pressure and steady-state-temperature conditions, the agreement was 0.04 %.

We have shown that a working standard comprised of a calibrated CFV, fast pressure and temperature sensors, and a heat exchanger can provide totalized mass flows with uncertainty  $< 0.15 \%$ . This makes it possible to use a CFV as a working standard to test the transient flow performance of other flowmeters that are being considered as

billing meters in gaseous fuel dispensers for hydrogen or natural gas. Figure 16 shows a test configuration that uses a CFV as a flow reference while subjecting a coriolis meter to flow, pressure, and temperature transients.

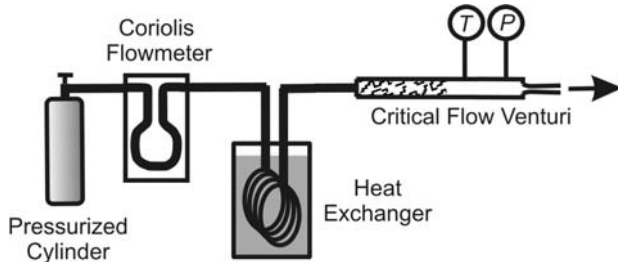
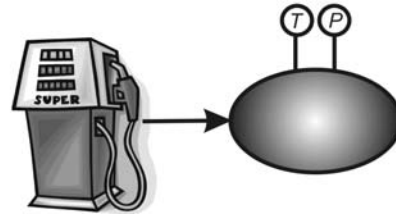


**Fig. 16** A test arrangement for laboratory evaluation of a coriolis meter measuring transient flows.

CFVs are also a practical solution to the problem of how to perform field verification of gaseous fuel dispensers. Periodic checks of the dispensers are performed by weights and measures inspectors to avoid fraud. Three methods are under consideration as the reference during fuel dispenser inspections: gravimetric (weighing a pressure vessel before and after filling), volumetric (same method as used to obtain  $\Delta\rho V$  herein), and master meters. The gravimetric and volumetric methods are cumbersome to apply in the field. For the gravimetric method, it is difficult to obtain low uncertainty measurements of the mass change in a heavy pressure vessel before and after filling with a low density gas. For the volumetric method, heat of compression makes it difficult to obtain a low uncertainty average temperature of the gas in the full tank, unless the tank is of a specialized design that promotes heat exchange.

The results in this paper show that a test procedure that uses a CFV as a master meter is viable (see Figure 17). The dispenser under test is used to fill a tank from an initial low pressure to high pressure (step 1). The tank is then discharged through a heat exchanger and CFV master meter until it is emptied to the initial pressure (step 2). The totalized mass flow from the CFV (plus a small correction for the change in gas density in the tank due to temperature change) is the reference value for checking the dispenser. This approach is cheaper, more compact, and more versatile than the gravimetric or volumetric methods.

Step 1) Fill tank via dispenser



Step 2) Empty tank through CFV

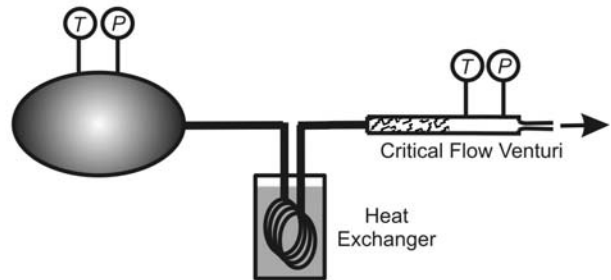


**Fig. 17** A CFV based field standard for conformance testing of gaseous fuel dispensers.

There are significant differences in the agreement between  $\int \dot{m} dt$  and  $\Delta\rho V$  depending upon whether there are transient or steady-state temperature conditions (-0.38 % versus 0.04 %). The difficulty in measuring the gas temperature entering the CFV seems the most likely cause of the disagreement under transient temperature conditions. Large temperature gradients and temporal temperature changes occur in many CFV applications due to gas cooling as it expands through pressure regulators and the CFV, conduction along the material walls, and heat transfer to the surroundings. Temperature sensors suffer from stem conduction errors and slow time response. In some cases these errors in temperature measurement cause significant flow measurement errors. We have found that much of the transient temperature problem is remedied by using a heat exchanger upstream. However, better temperature measurement approaches, such as placing small temperature sensors close to the CFV entrance, would permit accurate flow measurements without the bulk and expense of a heat exchanger.

## REFERENCES

- [1] Cascetta, F., Rotondo, G., and Musto, M., *Measuring of Compressed Natural Gas in*

- Automotive Application: A Comparative Analysis of Mass Versus Volumetric Metering Methods*, Flow Meas. Instrum., **19**, pp. 338 – 341, 2008.
- [2] ISO 9300, *Measurement of Gas Flow by Means of Critical Flow Venturi Nozzles*, Geneva Switzerland, 2005.
- [3] Wright, J. D., Johnson, A. N., Moldover, M. R., and Kline, G. M., *Gas Flowmeter Calibrations with the 34 L and 677 L PVTt Standards*, NIST Special Publication 250-63, National Institute of Standards and Technology, Gaithersburg, Maryland, (2004).
- [4] Lemmon, E. W., McLinden, M. O., and Huber, M. L., *Refprop 23: Reference Fluid Thermodynamic and Transport Properties*, NIST Standard Reference Database 23, Version 8.0, National Institute of Standards and Technology, Boulder, Colorado, April, 2007, [www.nist.gov/srd/nist23.htm](http://www.nist.gov/srd/nist23.htm).
- [5] Wright, J. D. and Johnson, A. N., *Uncertainty in Primary Gas Flow Standards Due to Flow Work Phenomena*, FLOMEKO, Salvador, Brazil 2000.
- [6] Wright, J. D. and Johnson, A. N., *Lower Uncertainty (0.015 % to 0.025 %) of NIST's Standards for Gas Flow from 0.01 to 2000 Standard Liters / Minute*, Proc. of the 2009 Measurement Science Conference, Anaheim, CA, 2009.
- [7] Johnson, A. N. and Wright, J. D., *Comparison between Theoretical CFV Flow Models and NIST's Primary Flow Data in the Laminar, Transition, and Turbulent Flow Regimes*, ASME J. of Fluids Eng., **130**, pp. 1-11, 2008.
- [8] Bignell, N. and Choi, Y. M., *Thermal Effects in Small Sonic Nozzles*, Flow Meas. Instrum., **13**, pp. 17 – 22, 2002.
- [9] Johnson, A. N., *Numerical Characterization of the Discharge Coefficient in Critical Nozzles*, Ph.D. Thesis, Pennsylvania State Univ., University Park, Pennsylvania, USA, 2000.
- [10] Wright, J. D., *Uncertainty of the Critical Venturi Transfer Standard Used in the K6 Gas Flow Key Comparison*, Proceedings of FLOMEKO, Johannesburg, South Africa, 2007.